

MESOPOROUS CARBON, VANADIUM PENTOXIDE, AND PRUSSIAN BLUE FOR ENERGY STORAGE: A PRELIMINARY STUDY

Tran Van Ket, Nguyen Van Tai, Vu Thao Trang, Tran Viet Thu*

Le Quy Don Technical University, Hanoi, Vietnam

Abstract

In this work, we present a preliminary study on the synthesis, characterization and electrochemical properties of three different nanoscale materials recently synthesized in our lab: mesoporous carbon (MPC), vanadium pentoxide (VPO), and Prussian Blue (PB). These materials were characterized using X-ray diffraction, scanning electron microscopy, cyclic voltammetry, and galvanostatic charge-discharge techniques. The electrochemical measurements revealed different behaviors for energy storage in these materials. The calculated values of specific capacitance for MPC, VPO, and PB at 10 mV s^{-1} was 149.1, 71.9, and 448.6 F g^{-1} , respectively, which are promising for electrochemical energy storage.

Keywords: *Mesoporous carbon; vanadium pentoxide; Prussian Blue; electrochemical energy storage.*

1. Introduction

Energy storage is the vital component for constructing sustainable energy systems [1]. Renewable energy produced from wind turbines and photovoltaics can produce energy in a sustainable manner; yet their intermittent nature still inhibits them from becoming a principal energy carrier. To offset this problem, energy storage technologies are being developed to store the generated intermittent energy and make it accessible upon demand. Along with the energy grid applications, the transportation systems and portable electronic devices also set additional requirements for power sources, such as higher energy density, improved durability, and lower cost [2]. Currently, the dominating power source remains the battery, mainly the lithium-ion batteries (LiB) [3]. LiB technology offers numerous advantages, including high energy density and long service life. However, the slow charge/discharge process in LiBs results in low power density (ca. $10\text{-}1000 \text{ W kg}^{-1}$) and short lifecycle (ca. 400-1200 cycles). Moreover, the high cost, limited resource, and reactive nature of lithium element have restricted their range of applications.

These disadvantages could be overcome with a different storage mechanism in power devices called supercapacitors [4, 5]. They are featured by high power density

* Email: thutv@mta.edu.vn

(typically 10 to 100 times greater than that of batteries), excellent durability, and high Coulombic efficiency [5]. However, supercapacitors also suffer from several shortcomings such as low energy density and high cost associated with the increased difficulty in producing high-performance materials [4, 5]. In order to bridge the gap between the potential and the commercial practicality of supercapacitor, recent research efforts have been focused on creating and improving the performance metrics of supercapacitor electrode materials [4].

The charging mechanism, electrochemical performance, and practical applications of a supercapacitor are mainly determined by its electrode materials. According to their energy storage mechanism, supercapacitors are classified into three types: (1) Electrochemical double-layer capacitors (EDLCs), in which electrolyte ions are electrostatically absorbed/desorbed from the electrodes with large specific surface area such as mesoporous carbon [6]. (2) Pseudocapacitors, in which electrical charges are transferred through chemical adsorption/desorption or redox reactions with linear potential-discharge time response. Some metal oxides such as ruthenium dioxide, manganese dioxide, and vanadium pentoxide belong to this category [7, 8]. (3) Battery-type supercapacitors, in which the charge storage is also faradaic in nature, but their charge/discharge curves display an apparent plateau feature [9]. Typical examples of these materials are transition metal oxides, sulfides, and Prussian Blue [10, 11]. Among these materials, mesoporous carbon, vanadium pentoxide, and Prussian Blue are attracting numerous research interests in recent years due to their promising performance [6, 10, 12]. However, these materials have been rarely studied by Vietnamese researchers.

In this work, we report on the synthesis, material characterization, and electrochemical properties of three different nanoscale materials recently synthesized in our laboratory: mesoporous carbon (MPC), vanadium pentoxide (VPO), and Prussian Blue (PB). Interestingly, we found that these materials exhibit different behaviors for energy storage corresponding to EDLC (for MPC), pseudocapacitor (for VPO), and battery-type supercapacitor (for PB). These materials were facilely synthesized using commercial chemicals and convenient laboratory facilities.

2. Experimental

2.1. Preparation of MSC, VPO, and PB samples

MSC was prepared by a two-step process. In the first step, indole (2.34 g) was reacted with excessive formaldehyde in a water-methanol mixture in the presence of $ZnCl_2$ for 24 hrs, then the dried at $105^\circ C$. In the second step, the obtained gel was calcinated at $450^\circ C$ for 1.5 hrs in nitrogen flow, and then the temperature was increased to

850°C and kept for 2 hrs. The obtained solid was washed with 1M HCl solution and deionized water until the filtrate become neutral, and dried in vacuum for 12 hrs.

VPO was prepared by the hydrothermal treatment of a solution containing ammonium vanadate (2.34 g), citric acid (2.28 g), and 105 mL deionized water at 160°C for 20 hrs. The resulting solid was dried at 60°C for 10 hrs, then calcined at 400°C for 2 hrs at a ramping rate of 2°C min⁻¹.

PB was prepared by the simple co-precipitation reaction between iron(III) sulfate (0.16 g) and potassium hexacyanoferrate(II) (0.76 g) in 40 mL water. After dissolving and mixing the above two reagents in water, the mixture was magnetically stirred for 3 mins and then aged at room temperature for 18 hrs. The resulting mixture was filtered and washed with water, then dried at 60°C for 6 hrs to obtain PB sample.

2.2. Material characterization

X-ray powder diffraction (XRD) patterns were obtained on a Bruker D8 Advance powder diffractometer with Cu K α X-ray radiation ($\lambda = 0.15418$ nm). Scanning electron microscopy (SEM) images of the samples were observed using a Hitachi SU70 microscope. Both the diffractometer and the microscope are equipped at Institute of Chemistry, Vietnam Academy of Science and Technology.

2.3. Electrochemical measurements

The electrodes were prepared by mixing active materials (MPC, VPO, or PB), conductive carbon, and binder (polyvinylidene fluoride) with a weight ratio of 7:2:1 in N-methyl-2-pyrrolidone. The resulting slurry was pasted on a Nickel foam and dried at 100°C for 24 hrs. The electrochemical measurements were carried out using Ag/AgCl reference electrode, Pt wire counter electrode, and 0.5M K₂SO₄ electrolytes on a Metrohm Autolab (PGSTAT 302N), equipped at Le Quy Don Technical University. The specific capacitance (C_s) was calculated from cyclic voltammogram (CV) curves using $C_s = (\int Idt)/(m\Delta V)$, where m is the weight of active material (g), I is the current (A), and ΔV is the potential window (V). The C_s was also calculated from galvanostatic charge-discharge (GCD) curves at different current densities using $C_s = (I\Delta t)/(m\Delta V)$, where I is the discharge current (A), and Δt is the discharge time (sec) [13-15].

3. Results and Discussion

3.1. Crystal structure

The XRD patterns of MPC (Fig. 1, bottom) could be well assigned to those of graphite (C, PDF #01-075-1621) with (002) and (100) lattice planes [14]. The XRD patterns of as-synthesized VPO samples (Fig. 1, middle) can be indexed to vanadium

pentoxide (V_2O_5 , PDF #01-076-1803) having orthorhombic crystal structure (space group $Pmn31$) with $a = 11.48 \text{ \AA}$ and $b = 4.36 \text{ \AA}$. Its major diffraction peaks could be assigned to the (200), (010), (101), (310), (301), (020), (002) and (012) lattice planes [8]. The XRD patterns of PB (Fig. 1, top) show that the as-prepared PB belongs to cubic system (space group $Fm-3m$) with $a = 10.13 \text{ \AA}$ (PDF #01-073-0687) and major diffraction peaks arising from (200), (220), (400), and (420) lattice planes of tetrairon tris(hexacyanoferrate) ($Fe_4[(Fe(CN)_4]_3$) [11]. The absence of other peaks indicates the synthesized MPC, VPO, and PB were phase-pure.

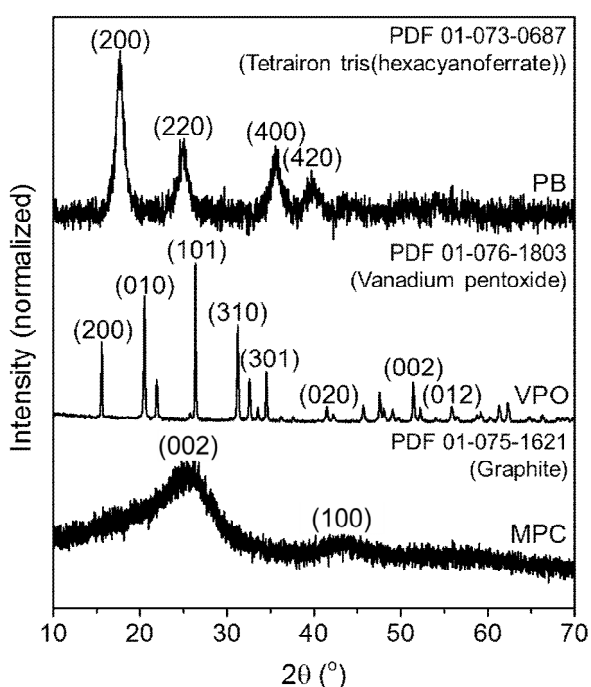


Fig. 1. XRD patterns of MPC, VPO, and PB.

3.2. Morphology

As shown in Fig. 2a, the MPC sample displays a network of carbon particles interconnected through open channels and mesopores of various sizes. This morphology is desired for the convenient exchange of electrolyte ions. The VPO sample (Fig. 2b) composes of one-dimensional nanorods with length of a few micrometers, which might be beneficial for the electronic conductivity of the electrode. The PB sample (Fig. 2c) exhibits the formation of aggregates, possibly formed during the ripening step. Each aggregate contains a large amount of primary particles with nanometer size.

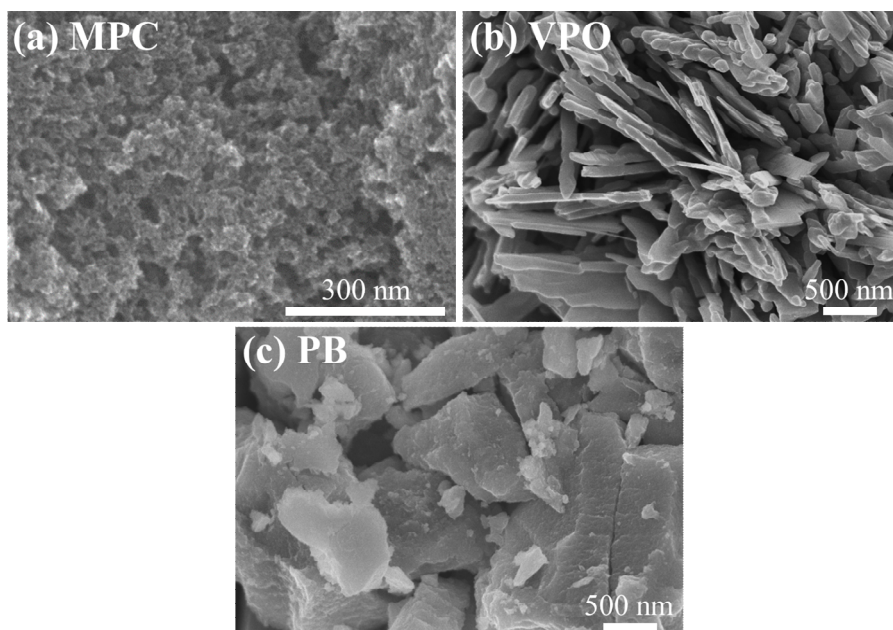
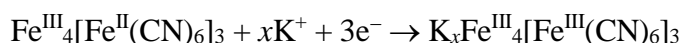


Fig. 2. SEM images of MPC (a), VPO (b), and PB (c).

3.3. Electrochemical properties

Fig. 3 shows the CV curves for all samples recorded at a scan rate of 10 mV s^{-1} . Interestingly, these samples displayed three different kinds of behavior which are typical for three types of supercapacitor electrode. The CV curve of PMC is closed to rectangular without any redox peaks, representing EDLC type within a limited potential window (-0.3 to 0.3 V). The CV curve of VPO indicate its pseudocapacitor behavior. In the CV curve of PB, a pair of well-defined redox peaks is clearly observed at *ca.* 0.24 and 0.02 V, which is attributed to the proposed redox reactions involved in the intercalation of electrolyte (K_2SO_4) with PB ($\text{Fe}^{\text{III}}_4[\text{Fe}^{\text{II}}(\text{CN})_6]_3$) as follows:



where K is the intercalated cation and K^+ is its corresponded cation in the solution. Also, PB can undergo a redox reaction between Fe^{3+} and Fe^{2+} in its structure. This suggests the PB materials display battery-type behavior due to Faradaic reactions [10, 16]. The CV curve for PB shows a much larger internal area than those of MPC and VPO, indicating that PB exhibits the largest C_s . The estimated C_s for MPC, VPO, and PB at 10 mV s^{-1} was 149.1, 71.9, and 448.6 F g^{-1} , respectively. The relatively high C_s for PB could be attributed to the high redox activity of the Fe(III)/Fe(II) centers in the material.

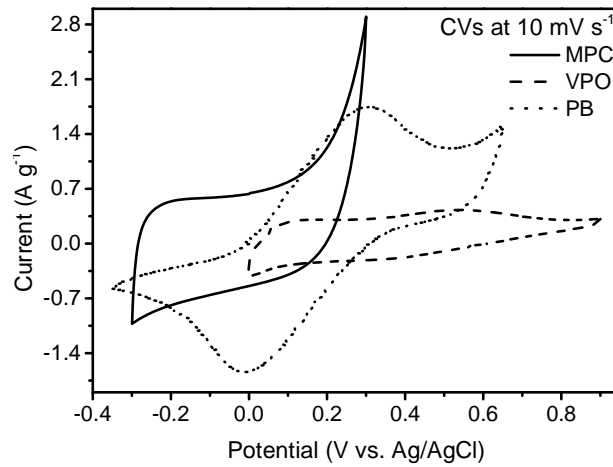


Fig. 3. CV curves of MPC, VPO, and PB at a scan rate of 10 mV s^{-1} .

Fig. 4 shows the GCD curves of MPC, VPO, and PB at a current density of 1 A g^{-1} . Their corresponding potential windows were 0.55 V (-0.3 to 0.25 V), 0.9 V (0 to 0.9 V), and 1.0 V (-0.35 to 0.65 V). The discharging part of the GCD of MPC and VPO is nearly linear, indicating an EDLC or pseudo-capacitor behavior. The specific capacitance calculated from GCD result of MPC and VPO was 69.4 and 54.6 F g^{-1} , respectively. While the C_s of MPC is typical for that of mesoporous carbon, the C_s of VPO is acceptable as compared to that of V_2O_5 nanobelts [8]. On the contrast, the discharging part of the GCD of PB clearly displayed a plateau centered at ca. 0.45 V (vs. Ag/AgCl), indicate a battery-type behavior. The calculated C_s of PB was 70.2 F g^{-1} at 1 A g^{-1} , which needs to be improved for practical applications.

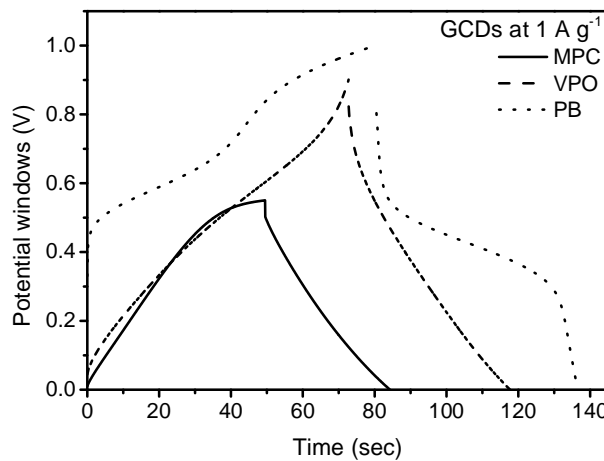


Fig. 4. GCD curves of MPC, VPO, and PB at a current density of 1 A g^{-1} .

4. Conclusions

This work provides convenient chemical routes to synthesize mesoporous carbon, vanadium pentoxide, and Prussian Blue for supercapacitor electrode. The as-synthesized materials exhibited well-defined crystal structure and morphology. They showed EDLC (for mesoporous carbon), pseudocapacitor (for vanadium pentoxide), and battery-type (for Prussian Blue) behavior for electrochemical energy storage. Although their C_s values were still lower than those of reported materials, there are plenty of rooms for improvements. Further efforts are being made including synthesis optimization, full cell assembly and testings.

Acknowledgement

The authors acknowledge the National Foundation for Science and Technology Development (NAFOSTED) for financial support (Grant No. 103.02-2020.31).

References

1. Lund, H., et al. (2016). Energy storage and smart energy systems. *International Journal of Sustainable Energy Planning Management*, 11, pp. 3-14.
2. Vazquez, S., et al. (2010). Energy storage systems for transport and grid applications. *IEEE Transactions on industrial electronics*, 57(12), pp. 3881-3895.
3. Scrosati, B., J. Hassoun, and Y.-K. Sun (2011). Lithium-ion batteries. A look into the future. *Energy Environmental Science*, 4(9), pp. 3287-3295.
4. Vangari, M., T. Pryor, and L. Jiang (2013). Supercapacitors: Review of materials and fabrication methods. *Journal of Energy Engineering*, 139(2), pp. 72-79.
5. Kim, B.K., et al. (2015). Electrochemical supercapacitors for energy storage and conversion. *Handbook of Clean Energy Systems*, pp. 1-25.
6. Prabakaran, S., R. Vimala, and Z. Zainal (2006). Nanostructured mesoporous carbon as electrodes for supercapacitors. *Journal of Power Sources*, 161(1), pp. 730-736.
7. Chen, D., et al. (2015). Ternary oxide nanostructured materials for supercapacitors: A review. *Journal of Materials Chemistry A*, 3(19), pp. 10158-10173.
8. Chen, D., J. Li, and Q. Wu (2019). Review of V_2O_5 -based nanomaterials as electrode for supercapacitor. *Journal of Nanoparticle Research*, 21(9), p. 201.
9. Zuo, W., et al. (2017). Battery-supercapacitor hybrid devices: Recent progress and future prospects. *Advanced Science*, 4(7), p. 1600539.
10. Zhao, F., et al. (2014). Cobalt hexacyanoferrate nanoparticles as a high-rate and ultra-stable supercapacitor electrode material. *ACS Applied Materials Interfaces*, 6(14), pp. 11007-11012.

11. Sun, H., et al. (2014). $\text{Fe}_4[\text{Fe}(\text{CN})_6]_3$: A cathode material for sodium-ion batteries. *RSC Advances*, 4(81), pp. 42991-42995.
12. Wu, C. and Y. Xie (2010). Promising vanadium oxide and hydroxide nanostructures: From energy storage to energy saving. *Energy Environmental Science*, 3(9), pp. 1191-1206.
13. Mai, L.-Q., et al. (2013). Synergistic interaction between redox-active electrolyte and binder-free functionalized carbon for ultrahigh supercapacitor performance. *Nature communications*, 4(1), pp. 1-7.
14. Thu, T.V., et al. (2019). Graphene- MnFe_2O_4 -polypyrrole ternary hybrids with synergistic effect for supercapacitor electrode. *Electrochimica Acta*, 314, pp. 151-160.
15. Van Nguyen, T., et al. (2020). Facile synthesis of Mn-doped NiCo_2O_4 nanoparticles with enhanced electrochemical performance for a battery-type supercapacitor electrode. *Dalton Transactions*, 49(20), pp. 6718-6729.
16. Yi, F., et al. (2020). Rational design of multiple prussian-blue analogues/NF composites for high-performance supercapacitors. *New Journal of Chemistry*, 44(25), p. 8.

CACBON XỐP, VANADI(V) OXIT, VÀ PRUSSIAN BLUE TRONG LƯU TRỮ NĂNG LƯỢNG: MỘT VÀI KẾT QUẢ BAN ĐẦU

Tóm tắt: Trong bài báo này, chúng tôi trình bày một số kết quả ban đầu về tổng hợp, xác định đặc trưng vật liệu và các tính chất điện hóa của ba loại vật liệu cấu trúc nano được chúng tôi tổng hợp gần đây: cacbon xốp (MPC), vanadi(V) oxit (VPO), và Prussian Blue (PB). Những vật liệu này được xác định đặc trưng bằng các kỹ thuật nhiễu xạ tia X, hiển vi điện tử quét, quét thế vòng tuần hoàn, và phóng nạp dòng không đổi. Các phép đo điện hóa đã cho thấy cơ chế lưu trữ điện tích khác nhau trong ba loại vật liệu này. Giá trị điện dung riêng tính được tại tốc độ quét 10 mV s^{-1} của MPC, VPO và PB lần lượt là 149,1; 71,9 và 448,6 F g^{-1} . Các giá trị này là tương đối khả quan cho lưu trữ năng lượng điện hóa.

Từ khóa: Cacbon xốp; vanadi(V) oxit; Prussian Blue; lưu trữ năng lượng điện hóa.

Received: 14/7/2020; Revised: 23/11/2020; Accepted for publication: 26/11/2020

